European Journal of Radiology Open 8 (2021) 100384

Contents lists available at ScienceDirect

European Journal of Radiology Open

journal homepage: www.elsevier.com/locate/ejro

Noninvasive prediction of pulmonary hemodynamics in chronic thromboembolic pulmonary hypertension by electrocardiogram-gated computed tomography

Fritz C. Roller [a,e,*], Selcuk M. Yildiz [a,e], Steffen D. Kriechbaum [b,e], Sebastian Harth [a,e], Andreas Breithecker [a,e], Christoph Liebetrau [b,e], Armin Schüßler [a,e], Eckhard Mayer [c,e], Christian W. Hamm [b,d,e,f], Stefan Guth [c], Gabriele A. Krombach [a,e], Christoph B. Wiedenroth [c]

[a] Department of Diagnostic and Interventional Radiology, University Hospital Giessen, Justus-Liebig-University Giessen, Klinikstraße 33, 35392, Giessen, Germany
[b] Department of Cardiology, Kerckhoff Heart and Thorax Centre, Bad Nauheim, Germany
[c] Department of Thoracic Surgery, Kerckhoff Heart and Thorax Centre, Bad Nauheim, Germany
[d] Department of Cardiology, University Hospital Giessen, Justus-Liebig-University Giessen, Klinikstraße 33, Giessen, Germany
[e] German Center for Lung Research (DZL), Giessen, Germany
[f] German Center for Cardiovascular Research (DZHK), RheinMain Chapter, Frankfurt am Main, Germany

HIGHLIGHTS

- Easily measurable parameters from chest CT examinations enable prediction of pulmonary hemodynamics.
- ECG-gated CTPA is superior to non-gated CT.
- Non-invasive pH therapy monitoring or follow-up might be implemented in the future.

ARTICLE INFO

Keywords:
Pulmonary hypertension
CTEPH
CTPA
Right heart catheterization

ABSTRACT

Purpose: The aim of the study was to investigate the potential of electrocardiogram (ECG)-gated computed tomography pulmonary angiography (CTPA) as a predictor of disease severity in patients with chronic thromboembolic pulmonary hypertension (CTEPH).

Method: Forty-five CTEPH patients with a mean age of 63.8 years±12.7 y (±standard deviation) who had undergone ECG-gated CTPA and right heart catheterization (RHC) were included in the study. Right ventricular to left ventricular volume ratio (RVV/LVV), diameter ratio on 4-chamber view (RVD4CH/LVD4CH), pulmonary trunk (PT) diameter, PT to aortic diameter ratio (PT/A), and septal angle were correlated to mean pulmonary artery pressure (mPAP). Moreover, RVV/LVV and RVD4CH/LVD4CH were adjusted to pulmonary diameter index (PADi) and PT/A index. Areas under the curve (AUC) for predicting mPAP above 40 mmHg, 35 mmHg, and 30 mmHg were calculated.

Results: RVD4CH/LVD4CH revealed the strongest correlation to mPAP before ($r = 0.6507$) and after ($r = 0.7650$; $p < 0.0001$) PT/A adjustment. The AUCs for predicting pH with mPAP over 40 mmHg and 30 mmHg were 0.9229 and 0.864, respectively. A cutoff value of 1.298 enabled prediction of pH with mPAP over 40 mmHg with a sensitivity, specificity, positive predictive, and negative predictive value of 80.00 %, 95.83 %, 88.46 %, and 94.12 %, respectively. Intra- and interobserver variability were excellent for all parameters.

Abbreviations: AUC, Area under the curve; CI, Confidence interval; CT, Computed tomography; CTEPH, Chronic thromboembolic pulmonary hypertension; CTPA, Computed tomography pulmonary angiography; ECG, Electrocardiogram; HU, Hounsfield units; ICC, intra-class concordance correlation coefficient; LV, Left ventricular; LVD, Left ventricular diameter; LVV, Left ventricular volume; MDCT, Multidetector computed tomography; mPAP, mean pulmonary artery pressure; NPV, Negative predictive value; PADi, Pulmonary artery diameter index; PH, Pulmonary hypertension; PPV, Positive predictive value; PT, Pulmonary trunk; RHC, Right heart catheterization; ROC, Receiver operating characteristics; RV, Right ventricular; RVD, Right ventricular diameter; RVV, Right ventricular volume; SD, Standard deviation; 4CH, four-chamber view.

* Corresponding author at: Department of Diagnostic and Interventional Radiology, University Hospital Giessen, Justus-Liebig-University Giessen Klinikstraße 33, 35392 Giessen, Germany.
E-mail address: fritz.c.roller@radiol.med.uni-giessen.de (F.C. Roller).

https://doi.org/10.1016/j.ejro.2021.100384
Received 11 August 2021; Accepted 11 October 2021
Available online 18 October 2021

Conclusion: Combining different and easily evaluable ECG-gated CTPA parameters enables excellent prediction of pulmonary hemodynamics in CTEPH patients. Ventricular diameter ratio on 4-chamber view adjusted by the PT/A ratio yielded the best correlation to mPAP.

1. Introduction

Pulmonary hypertension (PH) is defined as an elevation of mean pulmonary artery pressure (mPAP) greater than 20 mmHg according to the clinical classification that was updated 2019 [1]. Different etiologies of pH are known and have been categorized into five groups [2]. Chronic thromboembolic pulmonary hypertension (CTEPH) represents a subset of PH. In all pH etiologies morphologic changes with progressive right ventricular (RV) remodeling can be found. Initial RV myocardial hypertrophy due to emerging pressure overload and wall stress is followed by RV dysfunction and dilation [3]. Moreover, RV function deteriorates and RV diastolic pressure increases [4,5]. A progressive decline in stroke volume is triggered, and asynchronous or abnormal interventricular septal motion can be detected [6]. Due to the RV deterioration and abnormal septal motion, left ventricular (LV) filling and diastolic function also becomes impaired in the final stages of the disease.

Assessment of disease severity and morphology of pH is of importance for further risk stratification, treatment decision making, and outcome prediction. The gold standard diagnostic method in this setting is right heart catheterization (RHC), an invasive procedure that enables direct measurement of RV and pulmonary hemodynamics [7] with very low complication rates [8]. In contrast, echocardiography, a noninvasive option, permits evaluation of RV function but remains limited, as pulmonary pressures can only be estimated [7,9].

Computed tomography pulmonary angiography (CTPA), a further diagnostic method used in PH, can provide important information regarding cardiac and pulmonary vascular morphology, including the presence of acute or chronic embolism with mosaic perfusion pattern. CTPA has demonstrated low complication rates and investigator independence. Previous studies examined the performance of different morphologic CTPA criteria in the assessment of RV hemodynamics in pH patients. RV to LV volume and dimension ratios, pulmonary trunk (PT) to aortic diameter ratio (PT/A), septal angle, and other measurements were compared with RV function and pulmonary hemodynamics and showed promising correlations [10–13]. Moreover, Lim et al. adjusted the volume and dimension ratios according to the pulmonary artery diameter index (PADi) to reduce interference caused by the greater compliance of the RV compared with the relatively constant pulmonary diameter effect [10]. However, these studies differed significantly regarding CT technique utilized (ECG gated versus non-ECG gated) and underlying reference standard (RHC or echocardiography).

The use of ECG-gated CTPA and RHC provides the most thorough analysis of PH, because ECG-gated CTPA, with measurements performed within the same cardiac phase, is more accurate than standard CTPA, and, in contrast to the invasive measurement of mPAP via RHC, pulmonary pressure is often misjudged by echocardiography [14]. Therefore, we sought to investigate the performance of previously identified morphologic CTPA parameters for the assessment of pulmonary hemodynamics in a cohort of CTEPH patients who had undergone both ECG-gated CTPA and RHC. In addition, volume and diameter ratios were adjusted to PADi and PT/A to consider influences of both low- and high-pressure blood circulation systems.

2. Materials and methods

2.1. Study design

The study was performed as a retrospective data analysis. Parameters were analyzed by two independent readers (with 10 and more than 20 years of experience in cardiothoracic imaging, respectively) blinded to pulmonary hemodynamic parameters (mPAP). The study was approved by the local ethics committee (AZ 43/14) and all patients gave their written informed consent.

2.2. Study population

All consecutive CTEPH patients who had undergone ECG-gated CTPA for best possible delineation of thromboembolism prior to treatment and RHC between 2014 and 2017 were included. In addition, the diagnostic setup also included invasive pulmonary angiography, ventilation-perfusion scintigraphy, and echocardiography. ECG-gated multidetector CTPA was performed with two different CT scanner systems: initially, a first-generation dual-source CT scanner (Somatom Definiton, Siemens Healthineers, Forchheim, Germany) and, later, a third-generation dual-source CT scanner (Somatom Force, Siemens Healthineers, Forchheim, Germany) were used.

2.3. Right heart catheterization and computed tomography techniques

2.3.1. Right heart catheterization

Swan-Ganz RHC was performed via cubital or internal jugular vein by using a balloon-floating catheter, as described in detail [15]. pH was diagnosed if the mPAP was greater than 20 mmHg according to the updated clinical classification [1].

2.3.2. Computed tomography

The first-generation dual-source CT acquisition parameters were as follows: retrospective ECG gating (pulsing with preference at 70 % of the RR interval), craniocaudal direction from supraclavicular level to diaphragm, collimation 64 × 0.6 mm, rotation time 0.33 s, use of dose modulation systems (tube current modulation; CareDose, Siemens Healthineers, Forchheim, Germany).

The third-generation dual source CT acquisition parameters were as follows: prospective ECG gating (adaptive cardio sequence; pulsing with preference at 70 % of the RR interval), craniocaudal direction from supraclavicular level to diaphragm, collimation 152 × 0.6 mm, rotation time 0.25 s, use of dose modulation systems (tube current modulation and tube voltage adaption; CareDose; Siemens Healthineers, Forchheim, Germany), iterative reconstructions (Admire Level 4; Siemens Healthineers, Forchheim, Germany).

For both CT systems, 100 mL contrast medium (Ultravist 370; Bayer Healthcare, Berlin, Germany) was injected into an 18-gauge cubital vein catheter with a flow rate of 4 mL/s, followed by a 50-ml bolus of saline chaser. An automated bolus software program was used for the injection triggering (Care Bolus; Siemens Healthineers, Forchheim, Germany). The region of interest was placed in the pulmonary trunk and a threshold of 250 Hounsfield Units (HU) was used for initiating data acquisition. Image data were reconstructed with a slice thickness of 1.5 mm and 3.0 mm and an increment of 1.0 mm and 1.5 mm in angiographic and lung kernel. The dose length product was recorded for all examinations.

2.4. Evaluation of imaging parameters

2.4.1. Ventricular volume measurements

RV and LV volume measurements were performed using a standardized automated post-processing software (SyngoVia VB30A; Siemens Healthineers, Forchheim, Germany). After the automated ventricular volume measurements, all images were visually reviewed regarding precalculated ventricular borders. Manual corrections were performed when extraventricular structures were included or blood pool

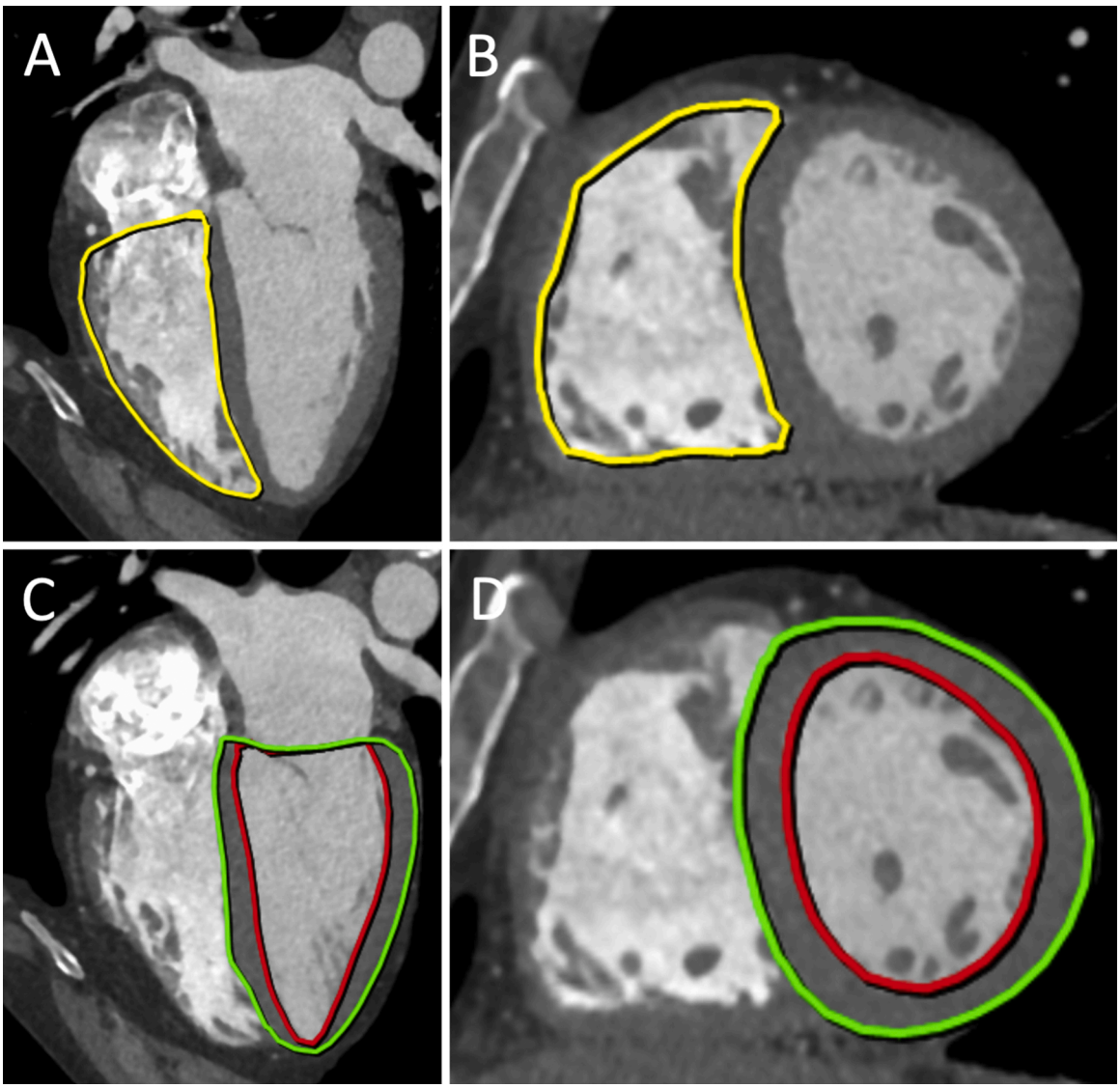

Fig. 1. Measurement of left and right ventricular volume.
The images present the software-assisted measurement of the left (Image C and D) and the right ventricular volumes (Image A and B) via precalculated and manually corrected endocardial borders. Red contours, left ventricular endocardial contour; green contours, left ventricular epicardial contour; yellow contours, right ventricular endocardial contour.

borders were inaccurate. Fig. 1 shows an example of right and left ventricular volume measurements (RVV/LVV).

2.4.2. Dimension measurements

Multiplanar reconstructions were used to measure the maximal distance between the ventricular endocardium and the interventricular septum for the RV and LV (RVD and LVD) in the 4-chamber view (4CH) (Fig. 2), and the RVD4CH/LVD4CH ratio was calculated. The maximum dimensions of the main pulmonary artery and the aorta were measured on axial CT sections with depiction of the main pulmonary artery bifurcation (Fig. 3). The septal angle was measured on axial CT sections (Fig. 4).

2.4.3. Pulmonary artery diameter index

The PADi was calculated for all subjects by dividing the pulmonary artery diameter by the individual body surface area.

2.4.4. Observer analysis

Intraobserver and interobserver variability were analyzed for all parameters. Initially, the first investigator (10 years of experience in cardiothoracic imaging) analyzed all CT images without any clinical information. To assess intraobserver variability, the image analysis was repeated after a period of 14 days by the same investigator. Moreover, a second experienced investigator (20 years of experience in cardiothoracic imaging) who was also blinded to patient demographics performed all diameter and volume measurements to determine the interobserver variability.

2.4.5. Statistics

All statistical analyses were performed using SPSS statistical software version 23 (IBM, Armonk, NY, USA). Continuous variables with normal distribution are expressed as mean ± standard deviation (SD); categorical data are presented as number and percentage. The intraclass concordance correlation coefficient (ICC) was used to assess intraobserver and interobserver variability for all parameters (PADi; septal angle; pulmonary artery diameter; pulmonary artery diameter/aortic diameter; RVD4CH/LVD4CH; RVV/LVV). An excellent agreement was defined as ICC > 0.8.

The dimension and volume ratios were multiplied by PADi or the PT/A ratio to assess their performance as constant variables. All parameters

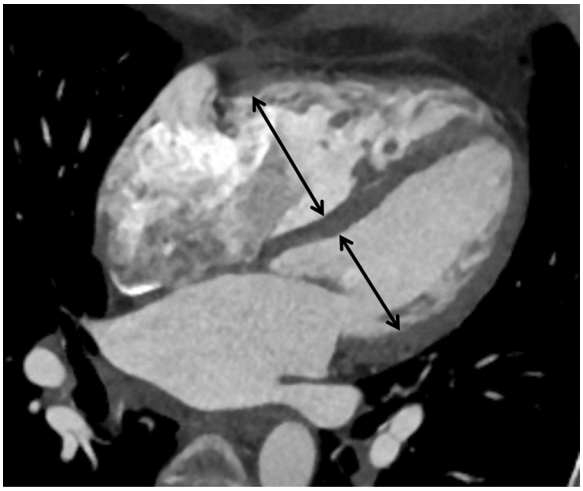

Fig. 2. Measurement of left and right ventricular diameter.
The image shows the measurement of the right and left ventricular diameters (arrows) in a four-chamber view (4CH) generated via multiplanar reconstruction.

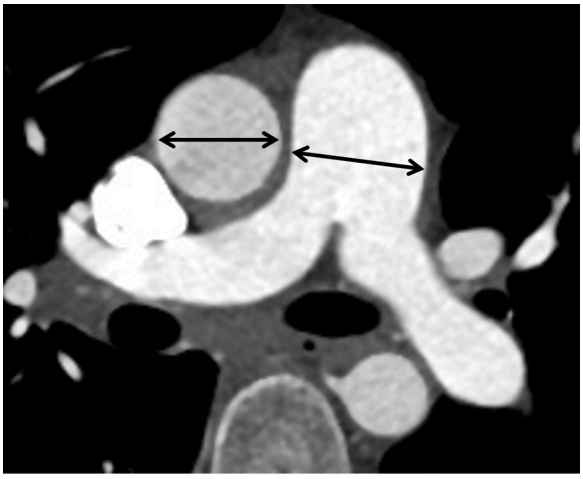

Fig. 3. Measurement of pulmonary trunk and aortic diameter.
The image shows the measurement of the pulmonary trunk and the ascending aortic diameter (arrows) on a transverse CTPA image at the height of the main pulmonary artery bifurcation.

were compared with mPAP using regression analysis with Pearson's correlation coefficient. The area under the curve (AUC) using receiver operating characteristic (ROC) analysis was calculated for the best correlating parameter to predict pH over 40 mmHg, pH over 35 mmHg, and pH over 30 mmHg. The results were tested at a 5% level of significance, and an alpha error of less than 0.05 was considered to be statistically significant.

3. Results

Forty-five patients (29 female) with a mean age of 63.8 years ± 12.7 y (range 30–80 years) were included in the study. The interval between ECG-gated CTPA and RHC was less than one week in all patients. Twenty-eight patients underwent ECG-gated CTPA and RHC within 2 working days (2.1 ± 3.3 days; range 0–7 days). The mean dose length products of the CT examinations were 386.7 ± 100.6 (5.8 ± 1.5 mSv) for the first-generation dual-source CT scanner in 28 patients and 189.0 ± 124.5 (2.8 ± 1.9 mSv) for the third-generation dual-source CT scanner in 17 patients.

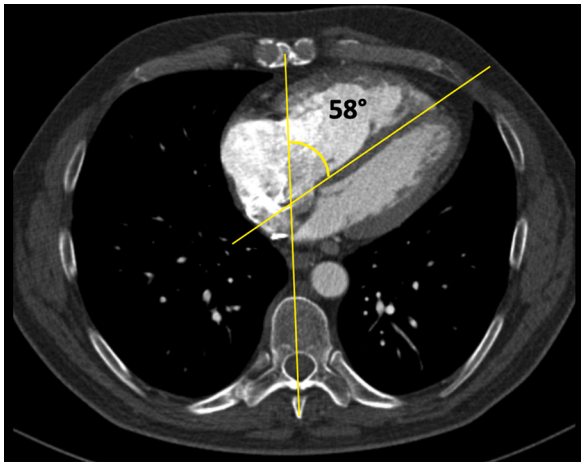

Fig. 4. Measurement of septal angle.
Septal angle measurement on a transverse CTPA image in a CTEPH patient. The septal angle is defined as the angle between the longitudinal axis of the vertebral body and the sternum or the xyphoid at the height of the transverse four-chamber view (4CH) with the axis of the septum.

Table 1
Baseline characteristics.

Patients	45
Sex, male : female	16 : 29
Age, years	63.8 ± 12.7
mPAP, mmHg	39.4 ± 12.1
≥ 40 mmHg	24 / 53.33
≥ 35 mmHg, < 40 mmHg	30 / 66.66
≥ 30 mmHg, < 35 mmHg	35 / 77.77

Values are mean ± SD or absolute values, n / %.
Abbreviation: mPAP – mean pulmonary artery pressure.

Table 2
CTPA parameters, mean values, and correlation to mPAP.

	mean +/- SD	r	95 % CI	p value
PT	32.49 ± 4.61	0.6083	0.3832 - 0.7652	< 0.0001
PT/A	1.06 ± 0.16	0.6172	0.3953 - 0.7711	< 0.0001
Septal angle	56.91 ± 14.79	0.3066	0.0143 - 0.5506	0.0405
RVD4CH/LVD4CH	1.45 ± 0.43	0.6507	0.4415 - 0.7928	< 0.0001
RVV/LVV	2.45 ± 1.37	0.5139	0.2595 - 0.7016	0.0003
PADi	17.72 ± 2.57	0.4371	0.1646 - 0.6475	0.0027
PADi x (RVD4CH/LVD4CH)	26.13 ± 9.58	0.6776	0.4794 - 0.8100	< 0.0001
PADi x (RVV/LVV)	44.33 ± 23.75	0.5514	0.3077 - 0.7273	< 0.0001
(PT/A) x (RVD4CH/LVD4CH)	1.57 ± 0.56	0.7650	0.6080 - 0.8644	< 0.0001
(PT/A) x (RVV/LVV)	2.63 ± 1.31	0.6541	0.4462 - 0.7950	< 0.0001

Abbreviations: PT – pulmonary trunk, A – aorta, RVD – right ventricular diameter, LVD – left ventricular diameter, 4CH – four chamber view, RVV – right ventricular volume, LVV – left ventricular volume, PADi – pulmonary artery diameter index, r – correlation coefficient, CI – confidence interval, p – significance value.

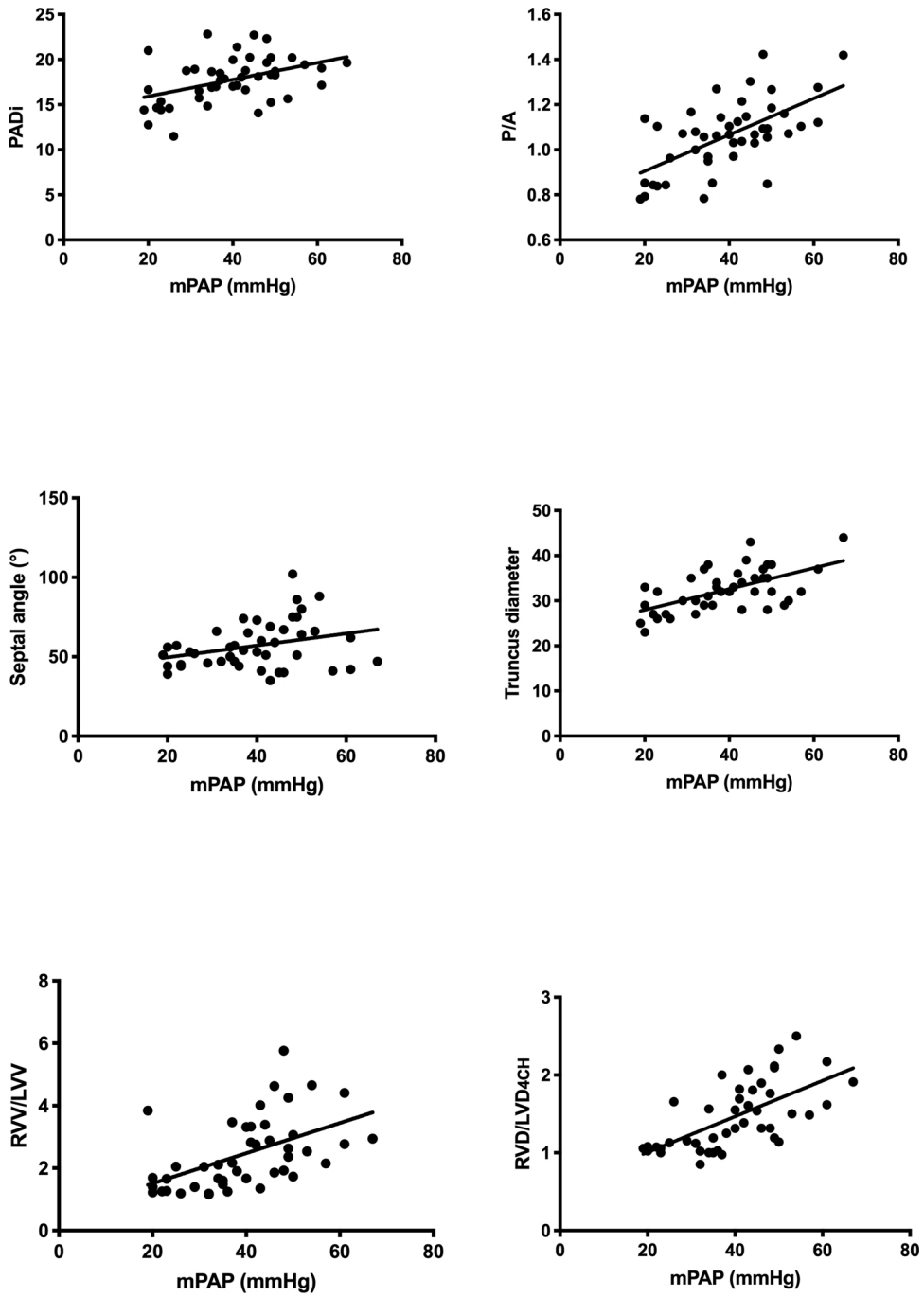

Fig. 5. Correlation of the different CTPA derived parameters to mPAP.

The mPAP was 39.4 ± 12.1 mmHg (range 21–67 mmHg) and the PVR was 568.9 ± 299.4 dyn x sec x cm^{-5} (range 131−1563 dyn x sec x cm^{-5}). Twenty-four CTEPH patients had an mPAP over 40 mmHg, thirty patients over 35 mmHg and thirty-five patients over 30 mmHg. Baseline characteristics are presented in Table 1.

The mean PT diameter (mm), PT/A, septal angle (°), PADi, RVD4CH/LVD4CH, and RVV/LVV were 32.49 ± 4.61, 1.06 ± 0.16, 56.91 ± 14.79, 17.72 ± 2.57, 1.45 ± 0.43, and 2.45 ± 1.37, respectively (Table 2). In our CTEPH study population the correlation between RVD4CH/LVD4CH and mPAP ($r = 0.6507$, $p < 0.0001$) was stronger than the correlation between PT/A and mPAP ($r = 0.6172$, $p < 0.0001$), PT and mPAP ($r = 0.6083$, $p < 0.0001$), RVV/LVV and mPAP ($r = 0.5139$, $p < 0.0003$), PADi and mPAP ($r = 0.4371$, $p < 0.0027$), or the septal angle and mPAP ($r = 0.3066$, $p < 0.0405$) (Fig. 5). After adjustment of RVV/LVV and RVD4CH/LVD4CH by PADi and PT/A, all correlations were increased and the product (RVD4CH/LVD4CH) x (PT/A) revealed the strongest correlation ($R = 0.7650$; $p < 0.0001$). Overall, parameter adjustment to PT/A revealed stronger correlations than adjustment to PADi. All correlations are demonstrated in Fig. 6.

The AUCs, confidence intervals, and p values for all parameters regarding prediction of pH over 40 mmHg are given in Table 3. The ROC curves and AUC values for the (RVD4CH/LVD4CH) x (PT/A) products are shown in Fig. 7. Comparing the AUCs of all parameters, the (RVD4CH/LVD4CH) x (PT/A) product had the greatest AUC, providing an excellent prediction of pH with mPAP over 40 mmHg ($p < 0.0001$). The AUC of (RVD4CH/LVD4CH) x (PT/A) for predicting mPAP over 40 mmHg was 0.923, for predicting pH over 35 mmHg was 0.901, and for predicting mPAP over 30 mmHg was 0.864 ($p < 0.0001$ for all

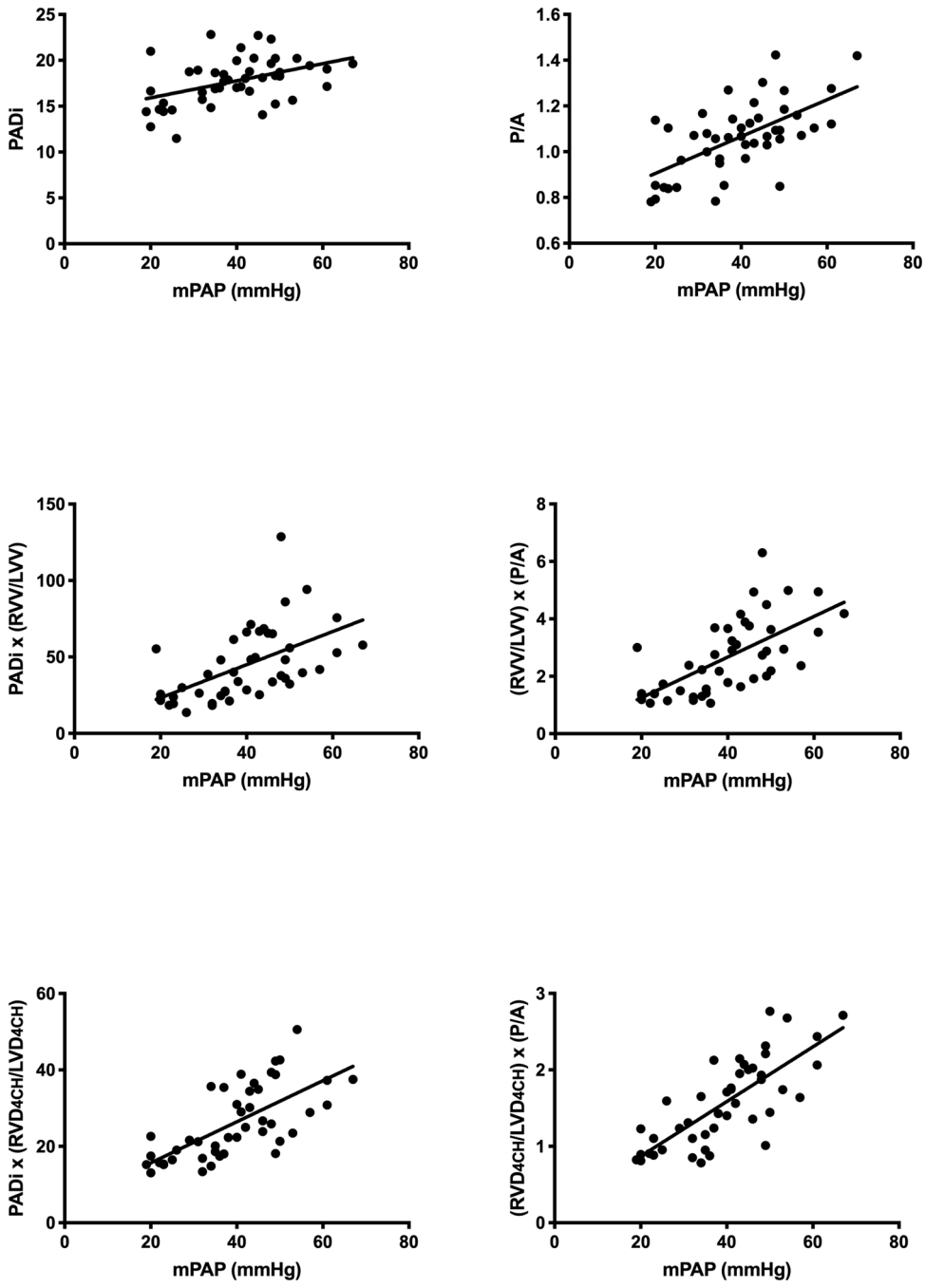

Fig. 6. Correlation of CTPA derived parameters after adjustment by PADi and PT/A.

comparisons) (Table 4).

When 1.298 was used as a cutoff value for (RVD4CH/LVD4CH) x (PT/A), the sensitivity, specificity, positive predictive value (NPV), and negative predictive value (PPV) for predicting pH with mPAP over 40 mmHg were 80.00 %, 95.83 %, 88.46 %, and 94.12 %, respectively (Table 4). With 1.335 as the cutoff value the sensitivity, specificity, PPV, and NPV for predicting mPAP over 35 mmHg were 88.67 %, 83.33 %, 92.59 %, and 73.68 %, respectively, and with 1.235 as the cutoff for mPAP over 30 mmHg these values were 90.00 %, 80.00 %, 96.55 %, and 56.25 %, respectively.

Excellent intra- and interobserver reproducibility were observed for determination of all parameters assessed. ICC values (intraobserver and interobserver) for PT were 0.9837 [95 % confidence interval (CI) 0.9698–0.9912] and 0.9785 (95 % CI 0.9588–0.9882), for PT/A 0.9529 (95 % CI 0.9140–0.9745 and 0.9513 (95 % CI 0.9112–0.9677), for septal angle 0.9512 (95 % CI 0.9236–0.9752) and 0.9506 (95 % CI 0.9298–0.9788), for RVD4CH/LVD4CH 0.9697 (95 % CI 0.9409–0.9845) and 0.9645 (95 % CI 0.9476–0.9898), for RVV/LVV 0.9781 (95 % CI 0.9602–0.9880) and 0.9698 (95 % CI 0.9570–0.9780).

4. Discussion

Over the last few decades new treatment options have significantly enhanced the outcome of pH patients. However, early diagnosis is still important to avoid advanced disease stages that are more difficult to treat and lead to a poor prognosis [16]. The present study was undertaken to investigate the performance of morphologic CTPA parameters for the assessment of pulmonary hemodynamics in a cohort of CTEPH patients who had undergone both ECG-gated CTPA and RHC. Our data demonstrates that a combination of different and easily evaluable

Table 3
AUC and p values for ROC predicting pH over 40 mmHg.

	AUC	95 % CI	p value
PT	0.7906	0.6557 - 0.9256	< 0.0010
PT/A	0.7948	0.6602 - 0.9294	< 0.0009
Septal angle	0.6542	0.4842 - 0.8241	0.0811
RVD4CH/LVD4CH	0.9073	0.8112 - 1.003	< 0.0001
RVV/LVV	0.8631	0.7487 - 0.9786	< 0.0001
PADi	0.7401	0.5900 - 0.8902	0.0049
PADi x (RVD4CH/LVD4CH)	0.9187	0.8316 - 1.006	< 0.0001
PADi x (RVV/LVV)	0.8869	0.7929 - 0.9809	< 0.0001
(PT/A) x (RVD4CH/LVD4CH)	0.9229	0.8391 - 1.007	< 0.0001
(PT/A) x (RVV/LVV)	0.9125	0.8272 - 0.9978	< 0.0001

Abbreviations: PT – pulmonary trunk, A – aorta, RVD – right ventricular diameter, LVD – left ventricular diameter, 4CH – four chamber view, RVV – right ventricular volume, LVV – left ventricular volume, PADi – pulmonary artery diameter index, AUC – area under the curve, CI – confidence interval, p – significance value.

ECG-gated CTPA parameters allows a good prediction of pulmonary hemodynamics in this patient group.

In routine clinical practice a multitude of tests and procedures, including echocardiography, RHC, ventilation/perfusion scintigraphy, CT, and cardiac MRI [17,18], are implemented in the diagnostic evaluation of pH patients. In this setting multi-detector computed tomography (MDCT) is commonly used to diagnose (acute or chronic) pulmonary embolism and parenchymal lung disease. In addition, changes in right heart pressure and/or right ventricular volume overload can be revealed by radiologic findings and morphologic cardiovascular features in CT. In particular, flattening or shifting of the interventricular septum, increased RV diameter or the RV-to-LV dimension ratio, and contrast material reflux to the inferior vena cava have been used to determine the severity of RV dysfunction and to predict outcomes in acute pulmonary embolism [19–26]. Moreover, multiple CTPA criteria for the assessment of pulmonary hemodynamic in pH were tested in different studies that showed promising results [10–13]. However, these studies are not comparable as they differ significantly regarding the CT technique utilized (ECG gated and non-ECG gated) and the underlying reference standard for assessment of RV and pulmonary hemodynamics (RHC or echocardiography). To obtain the best possible analysis, ECG-gated CTPA and RHC should be used: ECG-gated CTPA offers higher accuracy and standardization of performed measurements and RHC permits objective evaluation of pulmonary hemodynamics.

In line with the results of previous studies [10–13], our results showed promising correlations between different ECG-gated CTPA--derived parameters and pulmonary hemodynamic measurements and had excellent intra- and interobserver reproducibility. The weak correlation of septal angle to mPAP in our study cohort is comparable to that observed by (Tang et al. [12]), and the moderate correlation of pulmonary trunk to aortic diameter ratio (PT/A) is in line with previously published results [27]. In contrast to [10] the diameter ratio assessed in the 4-chamber view (RVD4CH /LVD4CH) was superior to the RV to LV volume ratio (RVV/LVV) and correlated more strongly to mPAP in our patients. Moreover, parameter adjustment by PADi, which was carried out with the goal of compensating for the high compliance of the RV to blood pressure and circulating blood volume, increased the correlations of RVV/LVV as well as RVD4CH/LVD4CH, as previously reported [10], confirming an incremental value of PADi. Therefore, we were able to demonstrate that combining all parameters with the PT/A ratio, to consider influences of the high- and low-flow blood circulating system, produces the best correlations. In particular, the combination PT/A x RVD4CH/LVD4CH was superior to the other parameters and showed the best correlation to mPAP (r = 0.7650). Furthermore, cutoffs for PT/A x RVD4CH/LVD4CH enabled discrimination of pH with mPAP over 40 mmHg, over 35 mmHg, and over 30 mmHg with a high and significant level of accuracy.

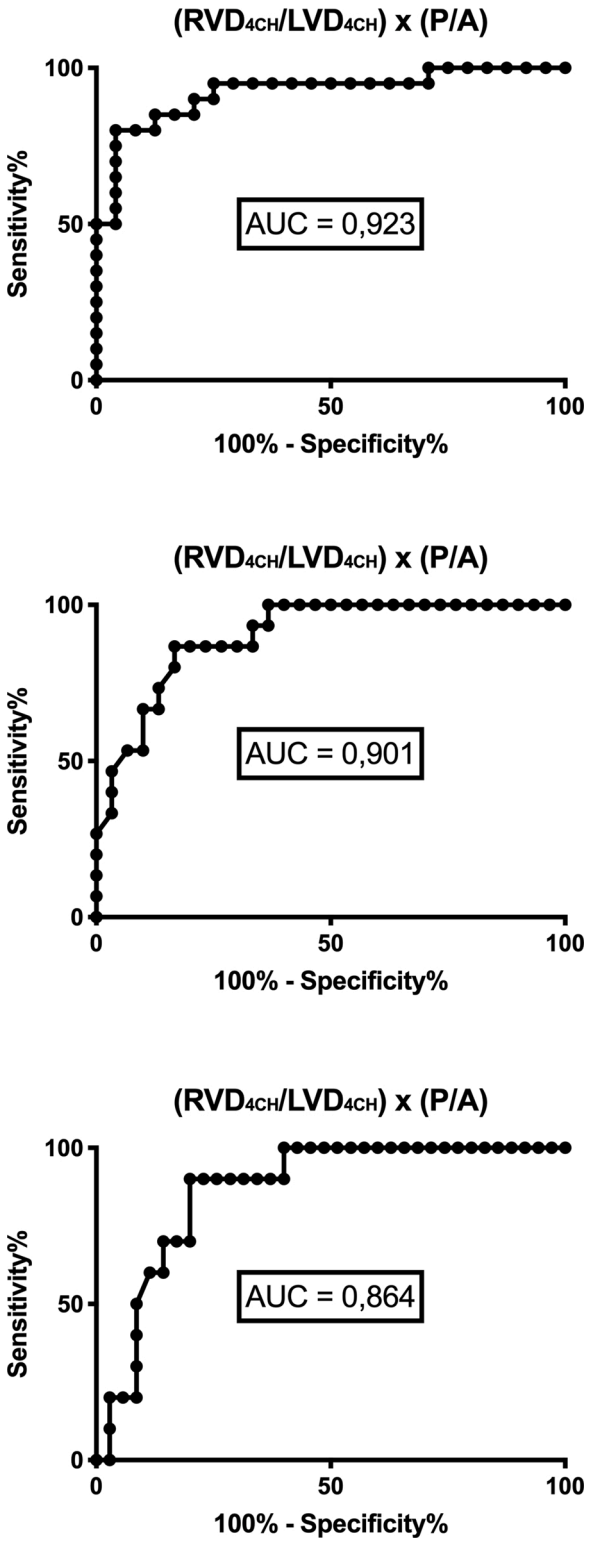

Fig. 7. ROC curves and AUC values for prediction of pH for (RVD4CH/LVD4CH) x (PT/A).

Several study limitations need to be acknowledged. First, the study is a retrospective data analysis of a small group of patients. However, a homogeneous CTEPH patient cohort was investigated in a standardized way and the time interval between invasive measurements of pulmonary hemodynamics and CTPA was very short. Further prospective studies with larger patient cohorts are needed to confirm our results. Second, the pathophysiologic considerations for determination of PADi, as

Table 4
(PT/A) x (RVD4CH/LVD4CH) ROC analysis for mPAP thresholds.

mPAP	Cut-off	Sensitivity	Specificity	PPV	NPV	AUC	P value
≥ 40 mmHg	1.298	80.00	95.83	88.46	94.12	0.923	0.0001
≥ 35 mmHg	1.335	86.67	83.33	92.59	73.68	0.901	0.0001
≥ 30 mmHg	1.235	90.00	80.00	96.55	56.25	0.864	0.0001

Abbreviations: mPAP – mean pulmonary artery pressure, ROC – receiver operating characteristics, PPV – positive predictive value, NPV – negative predictive value, AUC – area under the curve.

previously described [10], with differences in size changes for the RV and the pulmonary artery for a given volume or pressure change, were never assessed or quantified. This also applies to the PT/A ratio adjustment that was made to consider influences of the high- and low-flow blood circulating system on pH severity prediction. Nonetheless, we found that both adjustment methods led to improved correlations of all parameters with pulmonary hemodynamics, and therefore a certain degree of interdependence seems evident.

5. Conclusion

LV and RV diameter and volume ratios measured by ECG-gated CTPA showed good correlations to mPAP. Adjustment by PADi and PT/A ratio adds incremental value to all parameters, and RVD/LVD adjusted by PT/A (PT/A x RVD4CH/LVD4CH) showed the best correlation to mPAP and the highest accuracy for pH disease severity prediction.

Easily measurable parameters in ECG-gated chest CT examinations offer a great potential for pH assessment and for early identification of asymptomatic pH patients who may undergo chest CT examinations for unrelated reasons. Moreover, these parameters may facilitate non-invasive therapy monitoring or follow-up in the future.

Funding

Funded by the Deutsche Forschungsgemeinschaft (DFG), and the Collaborative Research Center (CRC) 1213, central project 01 (CP01).

Ethics approval and consent to participate

The study was approved by the local ethics committee (AZ 43/14) and all patients gave their written informed consent.

Authors' contributions

FCR, CBW and GAK were involved in study conception and design. FCR, SMY, SK, SH, AB, CL, AS, EM, CH, CBW and GAK contributed to acquisition of data. FCR, SMY, SK, SH, AB, CL, AS, EM, CH, CBW and GAK helped in analysis and interpretation of data. FCR, SMY, SK, SH, AB, CL, AS, EM, CH, CBW and GAK helped in drafting of manuscript. FCR, SMY, SK, SH, AB, CL, AS, EM, CH, CBW and GAK were involved in critical revision. All authors read and approved the final manuscript.

Declaration of Competing Interest

CBW has received speaker fees and/or consultant honoraria from Actelion, AOP Orphan Pharmaceuticals AG, Bayer AG, BTG, MSD, and Pfizer.

SG has received speaker fees from Actelion, Bayer, GSK, MSD and Pfizer.

The other authors declare that they have no competing interests.

Acknowledgements

We are grateful to Elizabeth Martinson, PhD, of the KHFI Editorial Office for her editorial assistance.

References

[1] G. Simonneau, D. Montani, D.S. Celermajer, et al., Haemodynamic definitions and updated clinical classification of pulmonary hypertension, Eur. Respir. 53 (1) (2019), 1801913.
[2] G. Simonneau, M.A. Gatzoulis, I. Adatia, et al., Updated clinical classification of pulmonary hypertension, J. Am. Coll. Cardiol. 62 (2013) 34–41.
[3] W.M. Bradlow, J.S. Gibbs, R.H. Mohiaddin, Cardiovascular magnetic resonance in pulmonary hypertension, J. Cardiovasc. Magn. Reson. 14 (6) (2012).
[4] G.E. D'Alonzo, R.J. Barst, S.M. Ayres, et al., Survival in patients with primary pulmonary hypertension. Results from a national prospective registry, Ann. Intern. Med. 115 (1991) 343–349.
[5] R.J. Raymond, A.L. Hinderliter, P.W. Willis, et al., Echocardiographic predictors of adverse outcomes in primary pulmonary hypertension, J. Am. Coll. Cardiol. 39 (2002) 1214–1219.
[6] C.M. Walker, J.H. Chung, G.P. Reddy, Septal bounce, J. Thorac. Imaging 27 (1) (2012). W1.
[7] N. Galie, M. Humbert, J.L. Vachiery, et al., 2015 ESC/ERS Guidelines for the diagnosis and treatment of pulmonary hypertension: The Joint Task Force for the Diagnosis and Treatment of Pulmonary Hypertension of the European Society of Cardiology (ESC) and the European Respiratory Society (ERS): Endorsed by: Association for European Paediatric and Congenital Cardiology (AEPC), International Society for Heart and Lung Transplantation (ISHLT), Eur. Heart J. 37 (1) (2016) 67–119.
[8] M.M. Hoeper, S.H. Lee, R. Voswinckel, et al., Complications of right heart catheterization procedures in patients with pulmonary hypertension in experienced centers, J. Am. Coll. Cardiol. 48 (2006) 2546–2552.
[9] M.R. Fisher, P.R. Forfia, E. Chamera, et al., Accuracy of Doppler echocardiography in the hemodynamic assessment of pulmonary hypertension, Am. J. Resp. Crit. Care Med. 179 (2009) 615–621.
[10] S. Lim, H. Lee, S.J. Lee, et al., CT signs of right ventricular dysfunction correlated with echocardiography-derived pulmonary arterial systolic pressure: incremental value of the pulmonary arterial diameter index, Int. J. Cardiovasc. Imaging 2 (2013) 109–118.
[11] H. Lee, S.Y. Kim, S.J. Lee, et al., Potential of right to left ventricular volume ratio measured on chest CT for the prediction of pulmonary hypertension: correlation with pulmonary arterial systolic pressure estimated by echocardiography, Eur. Radiol. 22 (9) (2012) 1929–1939.
[12] Q. Tang, M. Liu, Z. Ma, X. Guo, T. Kuang, Y. Yang, Non-invasive evaluation of hemodynamics in pulmonary hypertension by a Septal angle measured by computed tomography pulmonary angiography: Comparison with rightheart catheterization and association with N-terminal pro-B-type natriuretic peptide, Exp. Ther. Med. 6 (6) (2013) 1350–1358.
[13] N. Corson, S.G. Armato, Z.E. Labby, C. Straus, A. Starkey, M. Gomberg-Maitland, CT-based pulmonary artery measurements for the assessment of pulmonary hypertension, Acad. Radiol. 21 (4) (2014) 523–530.
[14] T.G. Flohr, S. Leng, L. Yu, et al., Dual-source spiral CT with pitch up to 3.2 and 75 ms temporal resolution: image reconstruction and assessment of image quality, Med. Phys. 36 (12) (2009) 5641–5653.
[15] C.B. Wiedenroth, A.J. Rieth, S. Kriechbaum, et al., Exercise right heart catheterization before and after balloon pulmonary angioplasty in inoperable patients with chronic thromboembolic pulmonary hypertension, Pulm. Circ. 10 (3) (2020), 2045894020917884.
[16] T.D. Nauser, S.W. Stites, Diagnosis and treatment of pulmonary hypertension, Am. Fam. Physician 63 (2001) 1789–1798.
[17] F.C. Roller, S. Kriechbaum, A. Breithecker, et al., Correlation of native T1 mapping with right ventricular function and pulmonary haemodynamics in patients with chronic thromboembolic pulmonary hypertension before and after balloon pulmonary angioplasty, Eur. Radiol. 29 (3) (2018) 1565–1573.
[18] F.C. Roller, C. Wiedenroth, A. Breithecker, et al., Native T1 mapping and extracellular volume fraction measurement for assessment of right ventricular insertion point and septal fibrosis in chronic thromboembolic pulmonary hypertension, Eur. Radiol. 27 (5) (2017) 1980–1991.
[19] P.A. Araoz, M.B. Gotway, J.R. Harrington, W.S. Harmsen, J.N. Mandrekar, Pulmonary embolism: prognostic CT findings, Radiology 242 (3) (2007) 889–897.
[20] G. Aviram, O. Rogowski, Y. Gotler, et al., Real-time risk stratification of patients with acute pulmonary embolism by grading the reflux of contrast into the inferior vena cava on computerized tomographic pulmonary angiography, J. Thromb. Haemost. 6 (9) (2008) 1488–1493.
[21] D. Collomb, P.J. Paramelle, O. Calaque, et al., Severity assessment of acute pulmonary embolism: evaluation using helical CT, Eur. Radiol. 13 (7) (2003) 1508–1514.

[22] A. Ghuysen, B. Ghaye, V. Willems, et al., Computed tomographic pulmonary angiography and prognostic significance in patients with acute pulmonary embolism, Thorax 60 (11) (2005) 956–961.
[23] R. Quiroz, N. Kucher, U.J. Schoepf, et al., Right ventricular enlargement on chest computed tomography: prognostic role in acute pulmonary embolism, Circulation 109 (20) (2004) 2401–2404.
[24] K.E. Lim, C.Y. Chan, P.H. Chu, Y.Y. Hsu, W.C. Hsu, Right ventricular dysfunction secondary to acute massive pulmonary embolism detected by helical computed tomography pulmonary angiography, Clin. Imaging 29 (1) (2005) 16–21.
[25] U.J. Schoepf, N. Kucher, F. Kipfmueller, R. Quiroz, P. Costello, S.Z. Goldhaber, Right ventricular enlargement on chest computed tomography: a predictor of early death in acute pulmonary embolism, Circulation 110 (20) (2004) 3276–3280.
[26] H. He, M.W. Stein, B. Zalta, L.B. Haramati, Computed tomography evaluation of right heart dysfunction in patients with acute pulmonary embolism, J. Comput. Assist. Tomogr. 30 (2) (2006) 262–266.
[27] E. Abel, A. Jankowski, C. Pison, J. Luc Bosson, H. Bouvaist, G.R. Ferretti, Pulmonary artery and right ventricle assessment in pulmonary hypertension: correlation between functional parameters of ECG-gated CT and right-side heart catheterization, Acta Radiol. 53 (7) (2012) 720–727.